Solid-State Characterization and Properties of Poly(*N*-methylcyclodisilazanes)

Hao Tang and Robert E. Prud'homme*

Centre de Recherche en Sciences et Ingénierie des Macromolécules, Chemistry Department, Laval University, Sainte-Foy, Québec G1K 7P4, Canada

Anne-Françoise Mingotaud, Michelle Schappacher, and Alain Soum

Laboratoire de Chimie des Polymères Organiques, Unité-Mixte CNRS, ENSCPB, BP 108, Avenue Pey Berland, 33402 Talence Cédex, France

Received August 12, 1996; Revised Manuscript Received January 7, 1997[⊗]

ABSTRACT: The solid-state structure and transition properties of three poly(*N*-methylcyclodisilazanes) were studied using differential scanning calorimetry (DSC), infrared (IR) and nuclear magnetic resonance (NMR) spectroscopies, dielectric relaxation, and X-ray diffraction techniques. Two endothermic transitions were observed in each of the DSC curves. It was found that the first transition, at lower temperatures, involves a change from a three-dimensional ordered phase to a two-dimensional ordered phase. This was shown by the disappearance or broadening of the intramolecular X-ray reflections, but also by the IR and NMR results, which show that the local mobility of the chain backbone and of several substituents increases significantly above the first transition temperature. This behavior can be achieved when going from a 3-D order where the chains are fixed in space one relative to the others to a 2-D order where the chains can move easily along the *c* axis. The second transition, at higher temperatures, is a melting transition according to X-ray and polarized microscopy results. The transition properties of the alternating copolymer are similar to those of the corresponding asymmetric homopolymer but its X-ray spectrum is close to that of the symmetric motif.

Introduction

Polysilazanes are organometallic polymers and promising candidates as precursors to ceramics or fibers usable at very high temperatures.[1−3] Duguet et al.[3] have shown that high molecular weight polysilazanes generally exhibit two endothermic transitions and a glass transition in the differential scanning calorimetry (DSC) curves. The high-temperature endotherm is the melting transition whereas the low-temperature endotherm can be attributed either to a conformational transition or to a crystal−crystal transition.

Similar transitions have been observed in several symmetric and asymmetric poly(*n*-alkylsilanes). At room temperature, it was found that dimethyl,[4,5] diethyl, di-*n*-propyl,[6] di-*n*-hexyl,[7−9] di-*n*-heptyl, and di-*n*-octyl[9,10] polysilanes have an all-trans, planar zigzag conformation, while a 7/3 helical conformation is observed in di-*n*-butyl[11] and di-*n*-pentyl[10−12] polysilanes; polymers having nonyl or longer side chains adopt a TGTG′ conformation.[10] As typical samples, poly(di-*n*-hexylsilane) (PDHS) and poly(dimethylsilane) (PDMS) have been examined extensively as a function of temperature. The PDHS backbone conformation is distorted above the phase transition temperature at 42 °C, primarily as a result of the disordering of the hexyl side chains, which involves changes both in the packing of the molecules and in the conformation of the silicon backbone. Similar results have been observed[7] for di-*n*-heptyl and di-*n*-octyl polysilanes, which show X-ray diffraction patterns[10] similar to that of PDHS. Contrary to PDHS, which exhibits changes in conformation and crystal structure at the first transition, PDMS shows two weak thermal transitions at 160 (ΔH = 10.9 J/g) and 220 °C (ΔH = 1.5−3.3 J/g). The first of these involves the retention of a trans conformation but the adoption of an orthorhombic packing on a hexagonal lattice. The second thermal transition involves additionally some conformational and orientational disordering.

In this study, DSC, IR and NMR spectroscopies, dielectric relaxation, and X-ray diffraction techniques have been used to determine the structure of three polysilazanes, at several temperatures below and above the endothermic transitions. Three poly(*N*-methylcyclodisilazanes) were used. They were prepared by anionic ring-opening polymerization of the corresponding cyclosilazane monomer.[3] Their chemical structure is

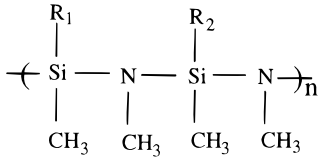

where R_1 = R_2 = CH_3 for poly(SiMe2), R_1 = R_2 = $CH{=}CH_2$ for poly(SiMeVi), and R_1 = CH_3 and R_2 = $CH{=}CH_2$ for poly(SiMe2−SiMeVi). The number-average molecular weights of poly(SiMe2), poly(SiMeVi), and poly(SiMe2−SiMeVi) are, respectively, 2500, 12000, and 38000. It is important to note that poly(SiMe2−SiMeVi) is truly an alternating copolymer since it was prepared from a monomer containing its two motifs.[3] Moreover, NMR spectroscopy indicates that more than 90% of the ring opening occurs in the same way.[3]

Experimental Section

DSC was carried out on a Perkin-Elmer DSC-7 apparatus at a heating rate of 10 °C/min under a dry nitrogen atmosphere. Calibration was performed using indium.

The specimens used for polarizing microscopy were prepared by casting tetrahydrofuran (THF) solutions onto a glass slide and drying in a vacuum oven at 30 °C for 2 days. The

[⊗] Abstract published in *Advance ACS Abstracts,* February 15, 1997.

S0024-9297(96)01209-0 CCC: $14.00

observations were made with a Carl Zeiss D-7082 microscope equipped with a Mettler FP-5 hot stage. The heating rate was 10 °C/min.

IR measurements were made on films of approximately 200 nm thickness, cast from a THF solution. The maximum absorption of the resulting films was lower than 1 absorbance unit, such that the spectra were within the linearity limit of the detector. A minimum of 100 scans at 2 cm^{-1} resolution was recorded on a Mattson Sirius 100 apparatus using a MCT detector. Elevated temperatures were obtained in a custom-made heating change that was calibrated with melting-point standards to ±1 °C.

^{13}C, ^{29}Si, and ^{15}N solid-state NMR spectra were recorded on a Bruker ASX 300 MHz NMR spectrometer equipped with a variable-temperature Bruker magic angle spinning probe and a ZrO_2 rotor. A sample spinning rate of 3.0−4.0 kHz and proton decoupling at a level of 45 kHz were employed. All the NMR spectra were obtained under magic angle spinning (MAS) conditions using dipolar decoupling with cross-polarization (CP). Solution NMR spectra were obtained from $CDCl_3$ solutions at a concentration of 40 mg/mL. Tetramethylsilane was used as a reference for the ^{13}C and ^{29}Si spectra and glycine-^{15}N for the ^{15}N spectra.

Films and powders were irradiated with a nickel-filtered Cu K_α X-ray beam from a Rigaku Model RU200B anode generator, at 55 kV and 190 mA. The temperature was controlled to within ±1.0 °C by a custom-made electrical heating device. Powder diffraction data were collected from as-received samples at a scan rate of 0.5−2.0°/min. For oriented films, a flat photographic film camera was used to record the diffraction patterns at several temperatures; exposure times varied from 30 to 60 min. Because the samples had a tendency to fracture during orientation, uniaxially drawn specimens of sufficient thickness for X-ray diffraction were prepared by a three-step procedure involving, first, casting films from a THF solution onto a flexible fluorinated ethylene−propylene copolymer substrate, second, drawing in an Instron tensile tester, and, third, removing the copolymer substrate. For the removal of the substrate, the drawn films were coated with a thick layer of poly(acrylic acid) gel in a 10% gel solution in water; after evaporation of the water, the glassy poly(acrylic acid) layer was peeled off the substrate together with the adhering polysilazane film and then, the poly(acrylic acid) layer was removed by repeated washings with distilled water. The oriented films were mounted with the draw axis parallel to the camera axis and perpendicular to the X-ray beam.

Results

1. Thermal Analysis. The first heating DSC scans of poly(SiMe2), poly(SiMeVi), and poly(SiMe2-SiMeVi) are shown in Figure 1. It can be seen that there are two endothermic peaks for each curve. For poly(SiMe2), the two transitions are centered at 154 (endothermic heat flow $\Delta H = 8.8$ J/g) and 226 °C ($\Delta H = 15.1$ J/g); for poly(SiMeVi), the two transition temperatures are at 67 ($\Delta H = 6.4$ J/g) and 136 °C ($\Delta H = 17.8$ J/g); and for poly(SiMe2-SiMeVi), two transition temperatures are found at 37 ($\Delta H = 5.0$ J/g) and 134 °C ($\Delta H = 10.7$ J/g). Moreover, the endothermic peaks of the copolymer are sharper than those of poly(SiMe2) and poly(SiMeVi), especially the upper one. It is finally noted that the transition enthalpy is always smaller for the low-temperature transition; in fact, it is roughly half the value of that of the high-temperature transition.

The higher transition temperatures of poly(SiMe2) as compared to poly(SiMeVi) can be attributed to the symmetry of its structure since its two substituents are the same, leading to a more stable crystal structure (the low molecular weight of poly(SiMe2) would suggest the opposite trend); similar trends have been observed with many other polymers, i.e., with polysilanes.[13−15] The lower transition temperatures of poly(SiMe2−SiMeVi) as compared to the two homopolymers can be attributed to its copolymer structure (its high molecular weight would suggest the opposite trend), giving a eutectic-like behavior, as seen in many other copolymers, such as poly(*n*-propylsilane-*co*-*n*-pentylsilane)[14] and poly(*n*-butylsilane-*co*-*n*-hexylsilane).[16]

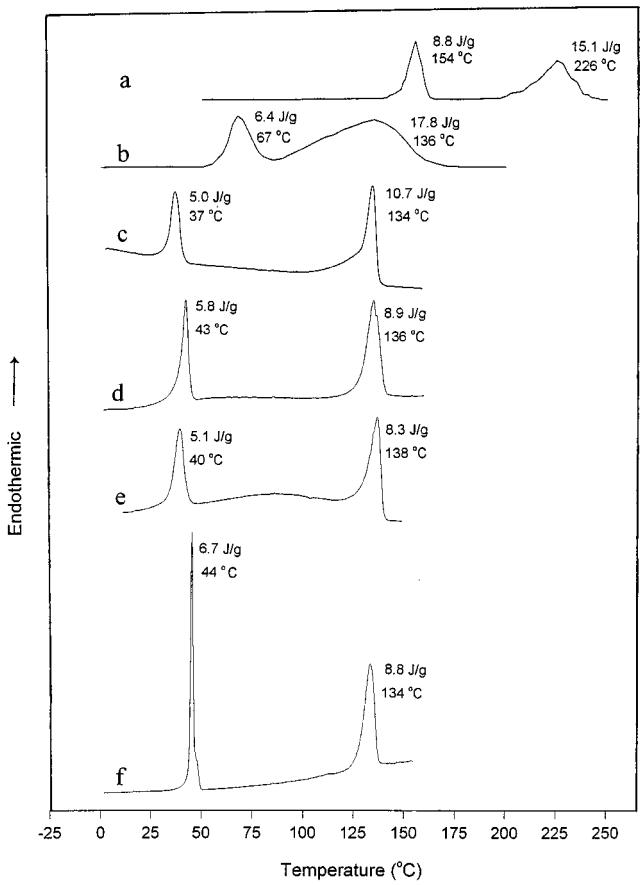

Figure 1. DSC analyses of (a) poly(SiMe2), (b) poly(SiMeVi), and (c−f) poly(SiMe2−SiMeVi). For the latter, the four scans correspond to (c) the original sample, (d) a heat treatment at 50 °C for 30 min, (e) a heat treatment at 100 °C for 30 min, and (f) a heat treatment at 140 °C for 30 min. Beside each peak are given the transition temperature and the transition enthalpy in J/g.

The effect of heat treatment on the transition behavior of poly(SiMe2−SiMeVi) is also shown in Figure 1. Samples d and e were kept at 50 and 100 °C for 30 min, i.e., in between the two transition temperatures, whereas sample f was heat treated at 140 °C, above the melting point (upper transition). It is seen that the two transition temperatures increase slightly after heat treatment at 50 and 100 °C and that the peak of the lower transition becomes sharper while the upper transition peak broadens slightly. In contrast, the heat treatment above the melting point (Figure 1f) leads to a very sharp low transition peak without any significant change in the upper transition peak. For the two homopolymers, however, the effect of heat treatment on the two transitions is weak.

2. X-ray Diffraction. The powder X-ray diffractograms of poly(SiMe2), poly(SiMeVi), and poly(SiMe2−SiMeVi), obtained at room temperature, are shown in Figure 2. It can be seen that the three polymers are semicrystalline. For poly(SiMeVi), there are two broad reflection peaks only centered at 11.9 and 26.5° (2θ). For poly(SiMe2) and poly(SiMe2−SiMeVi), however, a number of sharp peaks can be found, indicating a more ordered structure than in poly(SiMeVi). Moreover, most

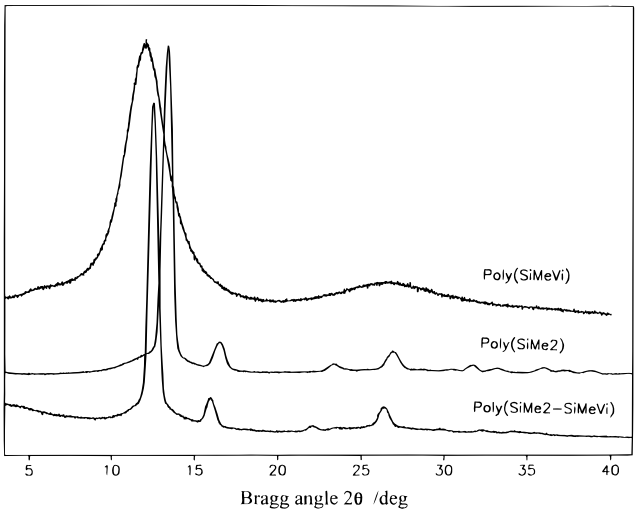

Figure 2. X-ray diffractograms of poly(SiMeVi), poly(SiMe2), and poly(SiMe2−SiMeVi) at room temperature.

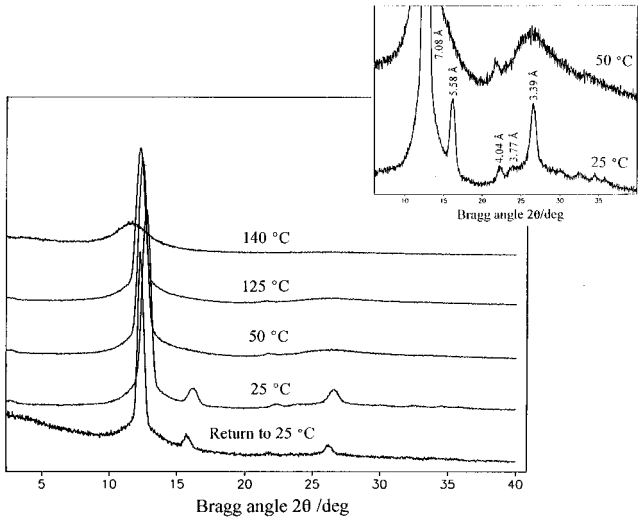

Figure 3. X-ray diffractograms of poly(SiMe2−SiMeVi) recorded at different temperatures. The insert shows a magnification of the intensity axis of the two spectra taken before and after the first transition.

reflections appearing in poly(SiMe2) can also be found in poly(SiMe2−SiMeVi) with a small shift in peak position. The less developed X-ray diagram of poly(SiMeVi) can be attributed to its asymmetric structure, which can be related to a certain extent to its lower transition temperatures (as compared to poly(SiMe2)) but also to its broad DSC peaks (although its transition enthalpies are of the same order of magnitude as those of poly(SiMe2)).

The X-ray diffraction patterns of poly(SiMe2−SiMeVi) at different temperatures are shown in Figure 3. The pattern obtained at 25 °C is dominated by several broad reflections centered at 7.08, 5.58, 4.04, 3.77, and 3.39 Å. At the low-temperature transition, between 25 and 50 °C, all reflections but the two at 7.08 and 3.39 Å smear out. However, the 7.08 and 3.39 Å peaks are not as sharp, particularly the latter, as they were before the transition. At 140 °C, the main reflection at 7.08 Å is reduced to an amorphous halo, centered at 12.5°, and all other reflections disappear (Figure 3). From studies on oriented films, it could be determined that the reflections at 7.08, 5.58, and 4.04 Å are equatorial whereas the reflections at 3.77 and 3.39 Å are meridional, even if the degree of orientation achieved was small. These equatorial reflections correspond, in first approximation, to intermolecular planes whereas the meridional reflections can be associated with intramolecular planes.

In polarized microscopy, as shown in Figure 4 for poly(SiMe2−SiMeVi), crystalline areas (birefringent spots) are clearly seen at room temperature, indicating that the polymer is semicrystalline. At 50 °C, above the first transition temperature, most birefringent spots that were present at room temperature remain, in agreement with the X-ray results showing that the main peak at 7.08 Å (and, to a certain extent, the 3.39 Å peak) retains its intensity at 50 °C. At 125 °C, however, some crystalline areas disappear, which coincides with the decrease of intensity of the intermolecular reflection centered at 7.08 Å seen in the X-ray spectra. Finally, no crystalline areas are left (the field is dark between crossed polars) at 140 °C, indicating that melting has occurred.

Figure 3 also shows the X-ray diffractogram of poly(SiMe2−SiMeVi) after a heating−cooling cycle. Compared with the original pattern at 25 °C, all the reflections have shifted to lower diffraction angles; i.e., the *d* spacings between chains increase by about 5%. Additional cycles led to the same spectrum, without any further change.

The X-ray spectra of poly(SiMe2) and poly(SiMeVi) at different temperatures are shown in Figures 5 and 6, respectively. For poly(SiMeVi), the broad peak centered at 3.45 Å is replaced by a broad amorphous-like background above the first transition temperature, whereas the main peak, centered at 7.35 Å, keeps its intensity until the second transition temperature. In the case of poly(SiMe2), however, the sharp reflection at 6.75 Å and several high-angle diffraction peaks (at 2.94, 2.46, and 2.16 Å) remain above the first transition temperature on top of the broad background peak. They are still there at 220 °C, near the second transition temperature.

3. Vibrational Spectroscopy. The IR spectra in the 1800−600 cm^{-1} region of poly(SiMe2), poly(SiMeVi), and poly(SiMe2−SiMeVi) are shown in Figure 7. It can be seen that several peaks in the copolymer, at 681, 795, and 1263 cm^{-1}, are also present in the two homopolymer spectra whereas others are shared by only one of the two homopolymers: the peaks at 834 and 1029 cm^{-1} are also present in poly(SiMe2) while those at 873, 950, 1060, 1185, 1406, and 1595 cm^{-1} are due to poly(SiMeVi).

The IR spectra of poly(SiMe2−SiMeVi) at different temperatures are shown in Figure 8. It is seen that there is a significant variation in intensity of the 1029 (C−N vibration, from the SiMe2 motif), 949, and 834 cm^{-1} ($\delta(CH_2)$ vibration from the SiMeVi motif) bands (relative to the intensity of the 1060 cm^{-1} band, which is due to the C−N vibration), whereas the variation in intensity of the other bands is smaller.

The ratio in intensity of the 1029/1060 and 950/1060 cm^{-1} bands during the first and second scans is shown in Figure 9 as a function of temperature. It is seen, in both cases, that the ratio decreases sharply at the transition temperature. From this figure, the transition temperature during the first and second heating scans can be determined at ca. 37 and 45 °C, respectively (the same value is found with the two bands reported), which are in good agreement with the 37 and 44 °C DSC values mentioned above. It is found, however, that the IR transition is steeper than that seen in DSC.

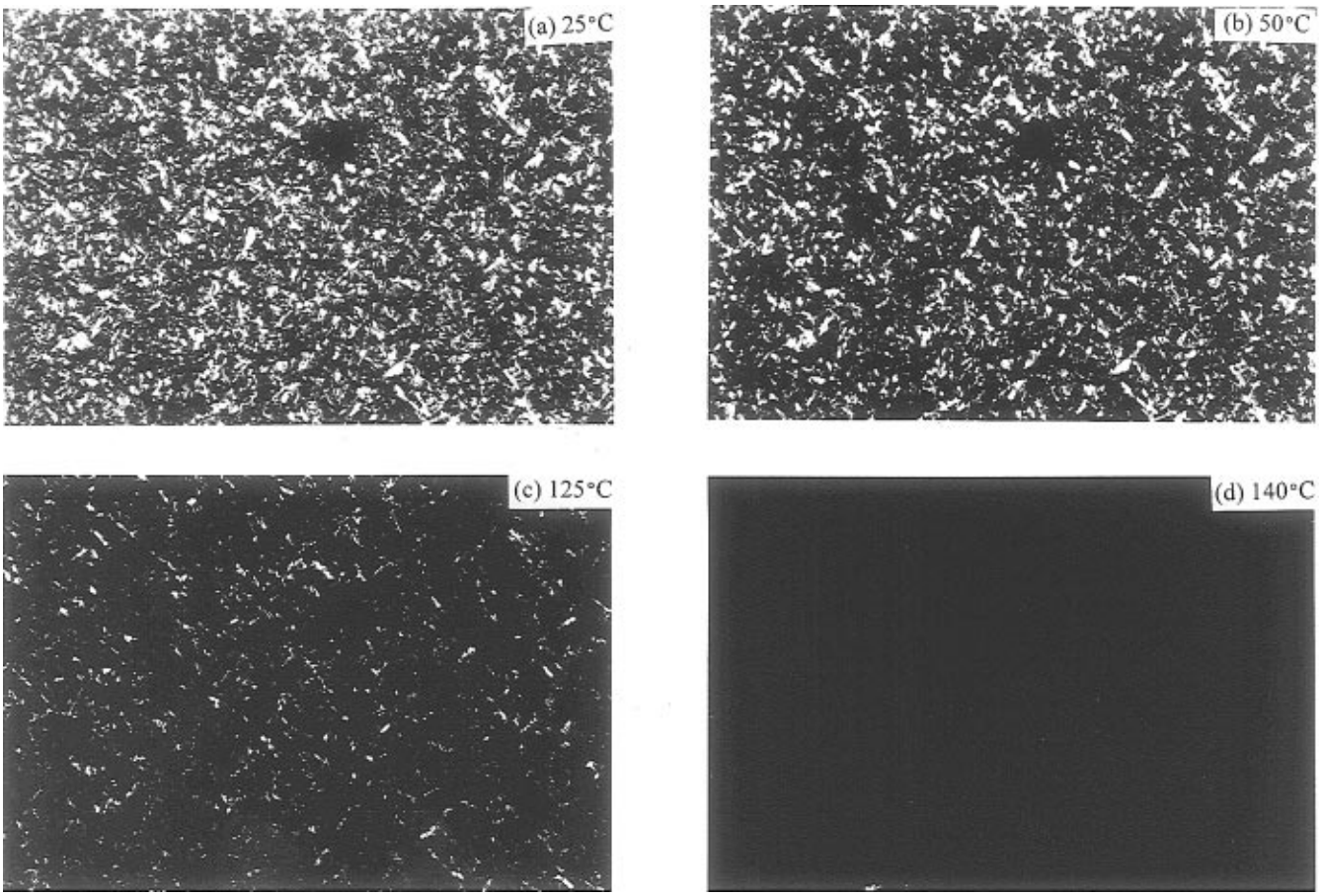

Figure 4. Micrographs of poly(SiMe2−SiMeVi) at (a) 25, (b) 50, (c) 125, and (d) 140 °C. The heating rate is 10 °C/min.

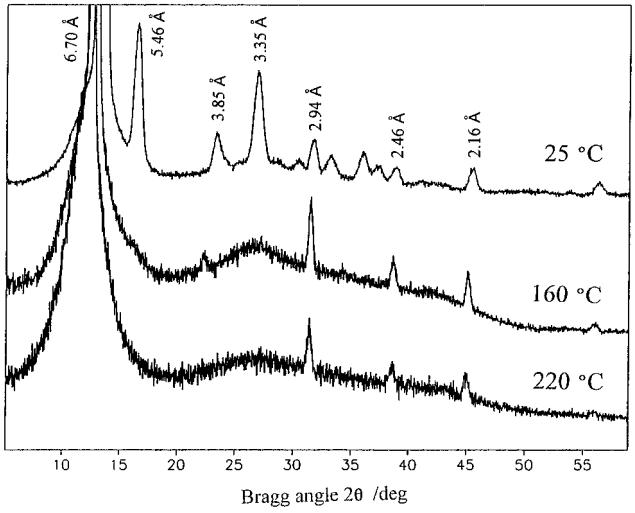

Figure 5. X-ray diffractograms of poly(SiMe2) recorded at different temperatures.

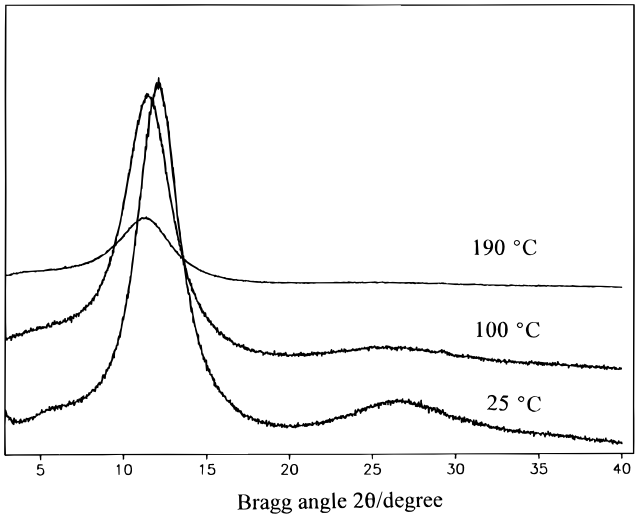

Figure 6. X-ray diffractograms of poly(SiMeVi) recorded at different temperatures.

We have also examined the UV and Raman spectra of poly(SiMe2−SiMeVi) at different temperatures. However, no UV absorption is found between 200 and 800 nm, contrary to the polysilanes,[11,16] and all the Raman peaks, including the Si−C stretch at 680 cm^{-1}, remain above the first transition temperature as compared to huge variations in intensity of the Si−C and Si−Si (410−510 cm^{-1}) stretch for polysilanes.[16]

4. NMR Spectroscopy. ^{29}Si, ^{15}N, and ^{13}C CP-MAS NMR spectra of poly(SiMe2−SiMeVi) obtainef at several temperatures are shown in Figures 10−12, respectively. In the ^{29}Si spectra, two resonance peaks with chemical shifts at −12.0 and −1.8 ppm are obtained, which can be assigned to the $CH_3-Si-CH_3$ and $CH_3-Si-CH=CH_2$ groups, respectively. Only one resonance peak is found in the ^{15}N spectra and it can be assigned to the CH_3-N groups. Finally, in the solid-state ^{13}C spectra, five resonance peaks are found with the assignments indicated in Figure 12 while, in the case of the solution spectrum, seven peaks are obtained since a splitting of the 2.6 ppm resonance peak occurs.

In all cases, there is a line narrowing occurring at the low transition temperature, i.e., between 25 and 50 °C. This suggests that, below the first transition temperature, the side chains (^{13}C resonances) and main chains (^{15}N and ^{29}Si resonances) exhibit little local motion; at

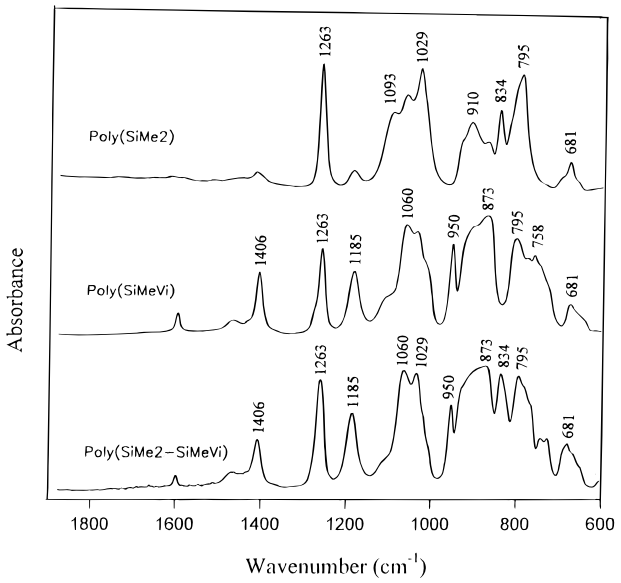

Figure 7. IR spectra in the 600−800 cm^{-1} region of poly(SiMe2), poly(SiMeVi), and poly(SiMe2−SiMeVi) at room temperature.

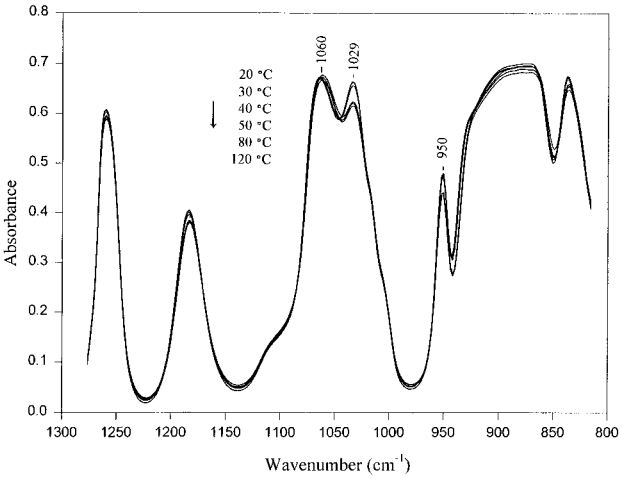

Figure 8. IR spectra in the 800−1300 cm^{-1} region of poly(SiMe2−SiMeVi) obtained at several temperatures between 20 and 120 °C.

50 °C, the motion in the side chains and main chains becomes larger on the NMR time scale such that differences of chemical environment and conformation are averaged. In solution, the side chains and main chains have an even larger local motion, resulting in an additional narrowing of the resonances and also in an obvious decrease in intensity.

Figure 13 shows the line width at half-height of Si, N, and C resonances as a function of temperature. In each case, the transition between 25 and 50 °C is clearly seen. It is interesting to note that the line width for ^{15}N at 50 °C is of the same order of magnitude as its solution counterpart, contrary to the ^{29}Si line width that remains larger, indicating a substantial increase in local backbone motion of nitrogen above the transition.

Figure 13 also shows that several peaks of ^{13}C resonances narrow down at the transition temperature like those of ^{29}Si and ^{15}N, whereas the 2.6 ppm peak (C-3, C-5, and C-7) remains nearly the same. Referring to the solution value, the 142 ppm peak (C-1) narrows significantly at the transition temperature while, for the 132 (C-2) and 31.2 ppm (C-4 and C-6) peaks, the line widths at 50 °C are between the values found at ambient

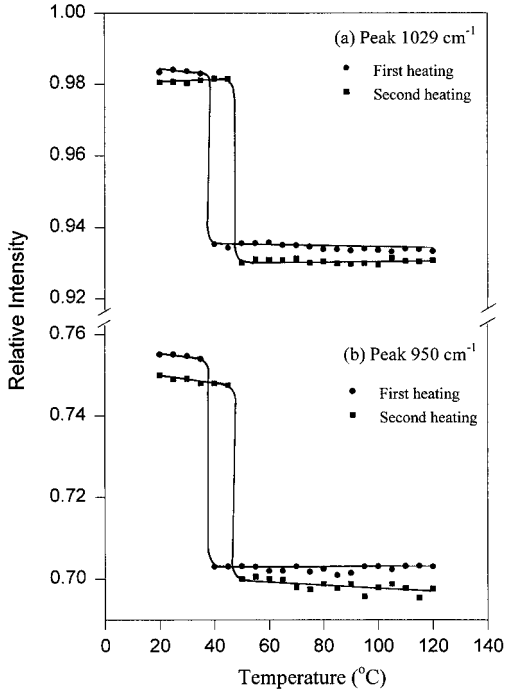

Figure 9. Intensity ratio of the (a) 1029 and (b) 950 cm^{-1} bands of the IR spectra of poly(SiMe2−SiMeVi), relative to the intensity of the 1060 cm^{-1} band, as a function of temperature for the first and second heatings.

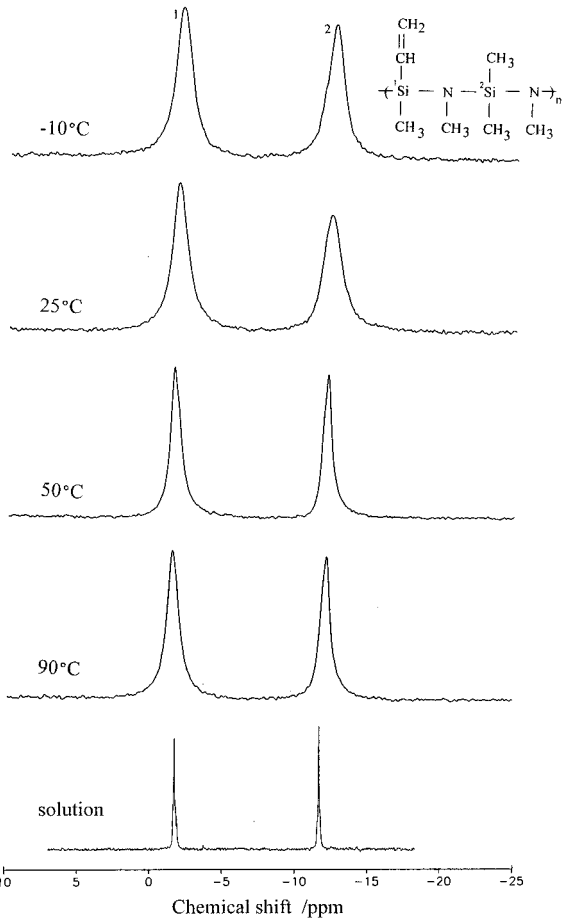

Figure 10. ^{29}Si CP-MAS NMR spectra of poly(SiMe2−SiMeVi) at several temperatures. The solution spectrum was taken at 25 °C in $CDCl_3$.

temperature or in solution. On the basis of these results, we can conclude that, above the first transition temperature, C-1, C-2, C-4, and C-6 have a substantial

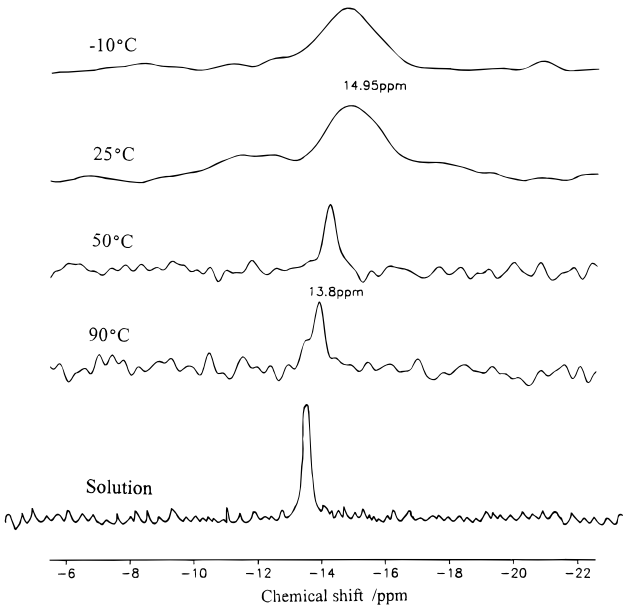

Figure 11. ^{15}N CP-MAS NMR spectra of poly(SiMe2−SiMeVi) at several temperatures. The solution spectrum was taken at 25 °C in $CDCl_3$.

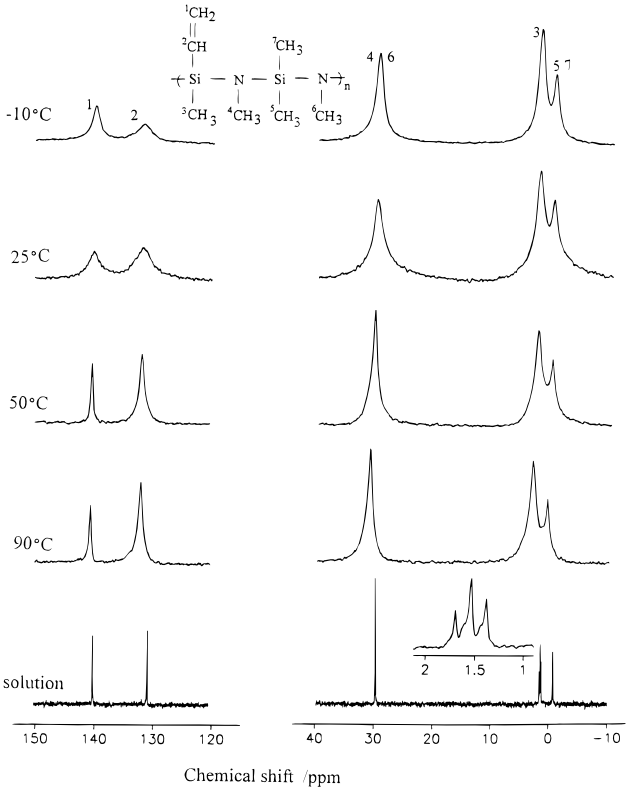

Figure 12. ^{13}C CP-MAS NMR spectra of poly(SiMe2−SiMeVi) at several temperatures. The solution spectrum was taken at 25 °C in $CDCl_3$.

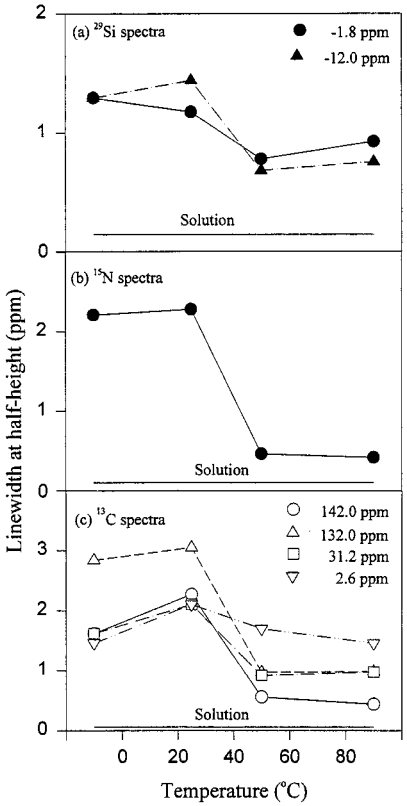

Figure 13. Line width at half-height of (a) ^{29}Si, (b) ^{15}N, and (c) ^{13}C resonances as a function of temperature for poly(SiMe2−SiMeVi). The straight line indicates the value of the corresponding solution spectra.

increase in local chain motion and more free volume. Compared with these nuclei, however C-3, C-5, and C-7 are relatively stable. In other words, the N−CH_3 groups gain in mobility, as well as the CH_2=CH substituent, but not the $SiCH_3$ group, except for a small narrowing of the ^{29}Si peak.

For poly(SiMe2−SiMeVi), we are not able to observe specific resonances for the crystalline and amorphous phases as was the case in PDHS.[10] It can be due to an overlap of the ordered and disordered phase resonances or to the small difference between the bond conformation of the side chains and main chains of those two phases. The fact that C, Si, and N chemical shifts show little change between the solid state (below and above the first transition temperature) and the solution indicates that there are only small differences in the average bond conformation of the side chains and main chains in those different conditions.

5. Dielectric Relaxation. Values of the tan δ (ϵ''/ϵ') at several frequencies for poly(SiMe2−SiMeVi) are plotted in Figure 14 as a function of temperature. The spectra exhibit a peak, centered at −50, −34, and −32 °C, respectively, for frequencies of 1, 7.5, and 50 kHz. According to the DSC results, this peak can be assigned as the glass transition relaxation. However, no relaxation peak could be found at the first transition. Figure 14 also shows the Arrhenius frequency−temperature plot of the glass transition relaxation, from which an activation energy of 59 kJ/mol is calculated. The polarity of hexamethyldisilazane models and of an amine-terminated poly(1,1-dimethylsilazane) oligomer was reported by Salon et al.[17] The loss tangent glass relaxation intensity of poly(SiMe2−SiMeVi) is of the same order of magnitude as that of the oligomer.

Discussion

On the basis of the DSC, optical microscopy, and X-ray results, it appears that the three polysilazanes investigated are semicrystalline at room temperature. DSC analyses also show that all three polymer samples exhibit two endothermic transitions. Let us consider first the low-temperature transition. Let us concentrate also on the copolymer behavior since more experiments have been made with this sample. The results shown in the previous section indicate that there are major changes occurring at this transition. First, several

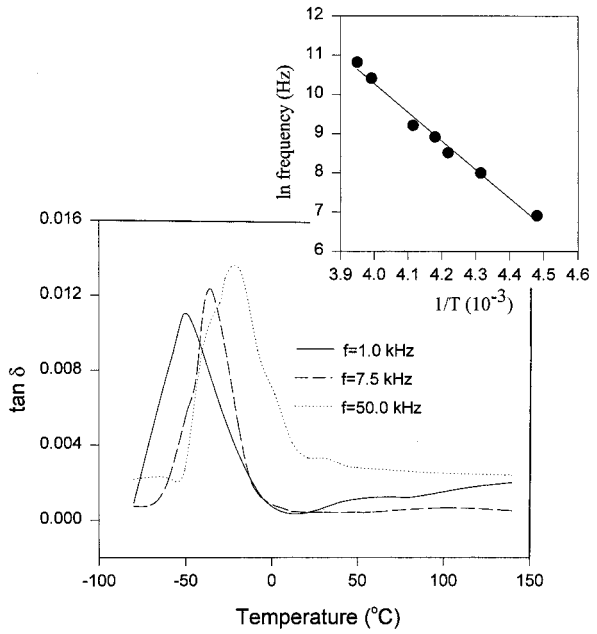

Figure 14. Dielectric tan δ as a function of temperature for poly(SiMe2−SiMeVi) at frequencies of 1.0, 7.5, and 50.0 kHz. The insert gives the Arrhenius plot of the glass transition relaxation.

X-ray reflections are lost (Figure 3). Second, several IR bands in the 850−1300 cm^{-1} region decrease in intensity (Figure 8), giving thus the opportunity to follow the transition (Figure 9). Third, the ^{13}C, ^{15}N, and ^{29}Si NMR peaks narrow significantly (Figures 10−12).

At the same time, the crystallinity of the material does not decrease much at this transition since minor changes are observed in polarized microscopy. Moreover, the loss of the intramolecular reflection at 3.77 Å and the important broadening of the intramolecular reflection at 3.39 Å suggest that the material went from a three-dimensional (3-D) order below the transition to a two-dimensional (2-D) order above the transition. This conclusion is also supported by the NMR results, which indicate that the local motion of several side chains (^{13}C peaks) and main chains (^{15}N and ^{29}Si peaks) increase significantly at this transition. In fact, there is an increase in mobility of the methyl groups attached to the nitrogen backbone atoms, and not those attached to the silicon atoms. Meanwhile, the loss of the two intermolecular reflections at 5.58 and 4.04 Å may be associated with a crystal structure change but additional data are needed to support this conclusion.

The increase in mobility and the disordering mentioned above can be associated with a change in conformation of the main chain, but not necessarily. It can also be associated with a change in crystal structure. At this moment, without more precise X-ray data, we cannot draw definitive conclusions. However, it is clear that the disorder observed involves a greater mobility of several of the side chains. This behavior can be achieved when going from a 3-D order where the chains are fixed in space one relative to the others to a 2-D order where the chains can move easily along the *c* axis. The actual X-ray data (Figure 3) support this possibility.

A comparison of the X-ray diffraction patterns of poly(SiMe2−SiMeVi) and poly(SiMe2) indicates that all the reflection peaks of the copolymer are found in poly(SiMe2), but at smaller Bragg diffraction angles. If this infers that the crystalline structure of poly(SiMe2−SiMeVi) is close to that of poly(SiMe2) (which still has to be demonstrated), it would imply that the unit cell of poly(SiMe2−SiMeVi) is bigger than that of poly(SiMe2), due to the SiMeVi repeat unit, which has a longer side chain than poly(SiMe2). In this context, it is noticed that the transition temperatures of poly(SiMe2−SiMeVi) are similar to that of poly(SiMeVi).

It is also interesting to compare the behavior of specific groups in the homopolymers and in the copolymer. We already emphasized the temperature effect of the 1029 cm^{-1} IR band in the copolymer which is due to the C−N vibration of the SiMe2 motif (Figure 7), allowing us to determine quantitatively the first transition temperature (Figure 9). However, we observed that this temperature effect is not present in the poly(SiMe2) spectra between room temperature and 100 °C. This difference indicates that the presence of a comotif (SiMeVi) in the copolymer increases significantly the mobility of the N−CH_3 group. A similar effect is seen in the ^{15}N NMR peaks of poly(SiMe2) and poly(SiMeVi), located at −13.5 and −15.5 ppm, respectively, which indicates that the environment of the nitrogen nucleus in poly(SiMe2) and poly(SiMeVi) is very similar, but not the same. However, as can be seen in Figure 11, the solid-state ^{15}N peak of poly(SiMe2−SiMeVi) at room temperature is broad because it includes both SiMe2 and SiMeVi components; i.e., the different environments of the nitrogen nuclei remain in the copolymer. This peak narrows significantly at 50 °C, suggesting that the nitrogen environment then becomes the same in the two repeat units due to the interaction of the side chains in the copolymer. Therefore, it may be concluded that there is an interaction between the side chains in the copolymer, by which the disordering of the N−CH_3 and Si−CH=CH_2 groups (in the SiMeVi sequence) has a significant effect on the N−CH_3 and CH_3−Si−CH_3 side chains (in the SiMe2 sequence).

Concerning the high-temperature DSC transition of poly(SiMe2−SiMeVi), it is seen that all the sharp peaks in X-ray diffraction and birefringent areas in polarized micrographs vanish at 140 °C. Hence, it can be concluded that this is a melting transition.

As mentioned in the Introduction, several polysilanes exhibit transitions similar to those described here for polysilazanes. For example, poly(SiMe2) can be compared to poly(dimethylsilane) (PDMS) since they have similar structures. Indeed, their transitions occur at similar temperatures: 154 versus 160 °C for the first transition, and 226 versus 220 °C for the second transition. Other comparisons become different due to the limited number of results available on poly(SiMe2). However, a more extensive comparison can be made between poly(SiMe2−SiMeVi) and PDMS. Poly(SiMe2−SiMeVi) goes from a 3-D to a 2-D order at the first transition whereas PDMS retains its 3-D order, but with a change in crystal structure. The disordering of the intramolecular planes of poly(SiMe2−SiMeVi) in comparison with PDMS may be caused by the fact that the Si−Si backbone in PDMS is replaced by a Si−N backbone in polysilazanes. In the case of polysilanes, the σ delocalization of electrons along the Si backbone makes the chain conformation very stable and unmodified at the first transition. For polysilazanes, however, the introduction of a nitrogen atom in the backbone leads to less σ delocalization of electrons, resulting in a more flexible chain. This increased flexibility makes the loss of the 3-D order possible at the first transition.

Conclusion

Semicrystalline polysilazanes exhibit two endothermic DSC transitions. At the low-temperature transition, it is found that the intramolecular X-ray reflections vanish or broaden, implying a change from a three-dimensional order to a two-dimensional order; meanwhile, several side chains and the main chain undergo increased local motions as evidenced by the IR and NMR spectra. However, it is not possible to confirm the presence of a conformational and/or crystal structure change at this transition. The high-temperature transition is clearly a melting transition since all the X-ray reflections and the crystalline regions seen under the polarizing microscope then vanish. The transition properties of poly(SiMe2−SiMeVi) are similar to those of poly(SiMeVi) but its X-ray spectrum is close to that of poly(SiMe2).

Acknowledgment. The authors acknowledge the Natural Sciences and Engineering Research Council of Canada and the Department of Education of the Province of Québec (FCAR program) for financial support. They also thank Claude-Paul Lafrance for his help in the X-ray analysis and Pierre Audet in the NMR studies.

References and Notes

(1) Laine, R. M.; Blum, Y.D.; Tse, D.; Glaser, R. *ACS Symp. Ser.* **1988**, *No. 360*, 142.
(2) Soula, G. *Actual. Chim.* **1988**, 249.
(3) Duguet, E.; Schappacher, M.; Soum, A. *Macromolecules* **1992**, *25*, 4835. Bouquey, M.; Brochon, C.; Bruzaud, S.; Mingotaud, A. F.; Schappacher, M.; Soum, A. *J. Organomet. Chem.* **1996**, *521*, 21. Soum, A.; Bruzaud, S. *Macromol. Chem.* **1996**, *197*, 2379.
(4) Patnaik, S. S.; Farmer, B. L. *Polymer* **1992**, *33*, 5127.
(5) Lovinger, A. J.; Davis, D. D.; Schilling, F. C.; Padden, F. J.; Bovey, F. A.; Zeigler, J. M. *Macromolecules* **1991**, *24*, 132.
(6) Lovinger, A. J.; Davis, D. D.; Schilling, F. C.; Bovey, F. A.; Zeigler, J. M. *Polym. Commun.* **1989**, *30*, 356.
(7) Lovinger, A. J.; Schilling, F. C.; Bovey, F. A.; Zeigler, J. M. *Macromolecules* **1986**, *19*, 2657.
(8) Patnaik, S. S.; Farmer, B. L. *Polymer* **1992**, *33*, 4443.
(9) Rabolt, J. F.; Hofer, D.; Miller, R. D.; Fickes, G. N. *Macromolecules* **1986**, *19*, 611.
(10) Karikari, E. K.; Farmer, B. L.; Miller, R. D.; Rabolt, J. F. *Macromolecules* **1993**, *26*, 3937.
(11) Schilling, F. C.; Lovinger, A. J.; Zeigler, J. M.; Davis, D. D.; Bovey, F. A. *Macromolecules* **1989**, *22*, 3055.
(12) Farmer, B. L.; Rabolt, J. F.; Miller, R. D. *Macromolecules* **1987**, *20*, 1167.
(13) Hallmark, V. M.; Sooriyakumaran, R.; Miller, R. D.; Rabolt, J. F. *J. Chem. Phys.* **1989**, *90*, 2488.
(14) Klemann, B.; West, R.; Koutsky, J. A. *Macromolecules* **1993**, *26*, 1042.
(15) Klemann, B.; West, R.; Koutsky, J. A. *Macromolecules* **1996**, *29*, 198.
(16) Bukalov, S. S.; Leites, L. A.; West, R.; Asuke, T. *Macromolecules* **1996**, *29*, 907.
(17) Salon, C.; Riande, E.; Fuentes, I.; Calleja, R. *J. Polym. Sci., Part B: Polym. Phys.* **1993**, *31*, 1591.

MA961209T